

CFD Analysis of the Combustion of Bio-Derived Fuels in the CFM56-3 Combustor

Jonas de Oliveira* and Francisco Brójo†

Universidade da Beira Interior, Covilhã, Castelo Branco, 6200-386, Portugal

A CFD simulation of a CFM56-3 combustor burning Jet-A and a 100% blend of biofuels, is performed. It is intended to evaluate the viability of these biofuels in a combustion point of view, by analyzing the emissions and the energy extracted when burning these through ICAO's LTO cycle, so that these biofuels can be considered as a future civil aviation fuel. The three biofuels considered for this study were extracted from Jatropha seeds, Algae and Sunflower. TAP kindly provided an operational CFM56-3 combustor, and with the aid of a 3D scanner, named Spider from Artec group, it was possible to create a 3D model of the combustor. From this 3D model, an STL file can be exported, and then imported into CATIA V5, which is the software chosen to perform the CAD. All of the relevant parts of the combustor are represented, which include the primary and secondary swirlers, fuel injectors, cooling holes, walls and the dome; only one quarter of the combustor was used for the numerical study due to the existing symmetry, and due to the fact that within the existing 20 fuel injectors, there are four of them that inject the fuel with a richer mixture. The numerical mesh is created using HELYX-OS and the commercial software FLUENT 15.0 is used to perform the numerical study. Due to the complexity of this study, the atomization of the fuel was not considered. The viscous model used is the RSM; all of the air-inlets as well as the fuel injectors are defined as mass-flow inlets, and the exit of the combustor is defined as a pressure-outlet. The final results show reasonable agreement with the reference values presented by ICAO, when Jet-A is combusted. The biofuel that presented the best performance in ICAO's LTO cycle regarding NO_x , CO and UHC emissions was sunflower biofuel, as these emissions were lower when compared to all of the fuels. Jatropha biofuel presented the highest CO_2 reduction, representing a 20% decrease from Jet-A, and the energy extracted represented a minimal decrease of 6% when compared to the same fuel. Overall, it can be concluded that the biofuels studied have the potential to replace kerosene, and despite more biofuel has to be burned to produce the same amount of energy as Jet-A, a significant reduction in emissions is predicted.

Nomenclature

CO	Carbon monoxide
CO_2	Carbon dioxide
EI	Emission index, $g_{emission}/kg_{fuel}$
\dot{m}	Mass flow rate, kg/s
NO_x	Nitrogen oxides
p	Static pressure, Pa
u	velocity, m/s

Abbreviations

AFR	Air to Fuel Ratio
CAD	Computer Aided Design
CFD	Computational Fluid Dynamics
CPU	Central Processing Unit

*Master Degree Student, Universidade da Beira Interior, Departamento de Ciências Aeroespaciais, Calçada Fonte do Lameiro

†Assistant Professor, Universidade da Beira Interior, Departamento de Ciências Aeroespaciais, Calçada Fonte do Lameiro, and AIAA 413414.

<i>FAMEs</i>	Fatty Acid Methyl Esters
<i>GHG</i>	Green House Gas
<i>GTE</i>	Gas Turbine Engine
<i>ICAO</i>	International Civil Aviation Organization
<i>LTO</i>	Landing and Take-Off
<i>LHV</i>	Lower Heating Value
<i>PZ</i>	Primary Zone
<i>RSM</i>	Reynolds Stress Model
<i>STL</i>	STereo Lithography
<i>TAP</i>	Transportes Aereos de Portugal
<i>UBI</i>	Universidade da Beira Interior
<i>UHC</i>	Unburned Hydrocarbons

Subscripts

<i>a</i>	air
<i>f</i>	fuel
<i>i, j, k</i>	direction vector

I. Introduction

In a world which the constant concern of global warming is an every day matter, the emissions that result from the combustion of fossil fuels is usually placed at the top as the main responsible for Greenhouse Gas (GHG) emissions, which are appointed as the primary factor that leads to global warming. The aviation industry by itself is responsible for around 3% of the total European Union (EU) GHG emissions, but the problem is that aviation is the only direct source of emissions into the upper atmosphere, and that these numbers are increasing fast, 87% since 1990.² Yet, darker forecasts are made by the International Civil Aviation Organization (ICAO), which predicts that by 2050 these emissions could grow up to 300%-700%.³ This increase in emissions drifts of course by the continuous increase of the demand of fuel, which in turn comes from the increase in the number of operational aircraft. In contrast, the resource of fossil fuel is depleting and will be finished in a near future. In fact, according to British Petroleum (BP), known oil deposits will only last until 2068, if we carry on this consumption rate.⁴

Fortunately, technology advances and practical solutions have been held to reduce the amount of heat-trapping emissions resultant by the continuous increase in traffic in the aviation industry. These solutions come in the form of protocols, improvements in aircraft structures/engines and alternative fuels. Examples of the first two solutions are the Kyoto protocol and the increase of the bypass ratio of turbofan engines, respectively; regarding this last, although changes like these did reduce the GHG emissions, they still present some problems. Modifications in aircraft components require a huge amount of money to take place; this is because these specific changed features has to be implemented in every single plane of the fleet, in order to achieve the desired reduction in GHG emissions. Another problem is the dependence in fossil fuels; these changes still do not resolve the fact that kerosene will no longer be available in the near future, due to the disappearance of known oil deposits. So changing the fuel source is one of the few options that remain for the aviation industry to reduce its GHG emissions.

The seek of a renewable drop-in fuel^a suitable for the aviation industry, comes as the best solution to resolve all the problems mentioned above. The environmental effects of any alternative fuel must be considered, this includes emissions from the engine and also life-cycle effects associated with the production and use of an alternative fuel.⁵ Safe and reliable operations of the engine must not be compromised in any way. Biofuel is a suitable choice which not only could significantly lower GHG emissions in up to 85%, if agro-pastoral land were to be used,⁶ but it is also a renewable fuel. Biomass derived from organisms, like *algae* and *jatropha curcas*, are the source of which future biofuels should be produced from. This is because, unlike biofuel produced after food crops, biomass derived from non-food crops do not enter in conflict with food resources. If the production of biofuel did enter in conflict with food resources, then there would be a big problem to deal with in the future.

^aA drop-in fuel is an alternative fuel that does not require adaptation of the fuel distribution network nor the engine fuel systems. It can be used without restrictions on aircraft or engine operability.

The main impact of trends and developments with the use of biofuels relative to combustor design, will be felt in fuel-nozzle design for multifuel capability, and in fuel/air management for minimum soot^b and gaseous emissions.⁷ These emissions include oxides of nitrogen (NO_x), unburned hydrocarbons (UHC), carbon monoxide (CO), Particulate Matter (PM) and oxides of sulfur (SO_x)^c. Although these pollutants do not contribute directly to global warming, they are hazardous to human health and therefore must be reduced. Carbon dioxide (CO_2) and water vapor (H_2O) are also products of the combustion process, but they are not regarded as pollutants because they are a natural consequence of the complete combustion of a hydrocarbon fuel. However, these two contribute to global warming and the only way to reduce them, is to burn less fuel.⁷

The problem of controlling emissions is complicated because of the fact that Gas Turbine Engines (GTE) operate over a wide range of power and ambient conditions. Aircraft engines have two requirements; the first is for very high combustion efficiency at low power, this is due to the large amount of fuel burned during taxiing and ground maneuvering, and the primary problem here is the reduction of UHC . At take-off power, climb and cruise the main concern are NO_x . ICAO sets standards on a worldwide basis, for both Landing and Take-off (LTO) cycles, and also for cruise at high altitude; the first is concerned with air quality in the regions surrounding airports, and the second with ozone depletion in the upper atmosphere.⁸

Research and development of biofuel for the aviation industry promises a prospect and interesting work, however it also issues many challenges due to the strict requirements of aviation fuel that are regulated by the American Society for Testing and Materials (ASTM). As these requirements are achieved, so as combustion products and the efficiency of these biofuels been correctly studied, the world takes a step closer to become less dependent of fossil fuels and mitigate global warming issues. This moment will come sooner than people think, and as the Saudi oil Minister Sheik Ahmed Zaki Yamani said in the 1970's, "The Stone Age did not end for lack of stone, and the oil age will end long before the world runs out of oil."⁹

A. Biofuels

Nowadays, there are a wide variety of alternative fuels, but all of them present some challenges to implement when compared to conventional jet fuel. However, among all of these alternatives, biofuels and in longer term hydrogen, have the potential to replace conventional jet fuel, as the first could be easily implemented in the present and future aircraft, thus being a drop-in fuel which would require little or no modification to current aircraft design.¹⁰ Biofuels can be defined as combustible liquids, that are manufactured from renewable sources such as plant crops. Crops with high oil content such as sunflowers, should be the starting point for any biofuel implementation, as these can produce high energy outputs.¹¹ This oil can be obtained by first cleaning, cracking and conditioning the beans. These oils are triglycerides of fatty acids, and the process of producing biofuel, involves a process named transesterification which applied to these triglycerides with methanol, produce the so called Fatty Acid Methyl Esters (FAMES). These FAMES are responsible for the close similarity to conventional jet fuel, as they have similar physical and chemical properties.¹⁰ The biofuels chosen for this work were from algae, jatropha and sunflower, and were done so taking into account their social, environmental and economical advantages. The jatropha biofuel FAMES composition was obtained from the work of Goyal et al.;¹² sunflower and algae biofuel FAMES composition, was obtained from the work of Sanford et al.¹³

Many place the land usage necessary to produce the required amount of biofuel as the main drawback for them to completely replace Jet-A. Regarding this particular subject, a study held by Boeing concluded that the land required to produce the required amount of biofuel for aviation, is in the order of 2.7×10^6 ,¹⁴ and with respect to this value, Australia by its own could easily produce the required amount of biofuel, from Jatropha feedstock. Moreover, as there is other places in the world were Jatropha could be grown, one can conclude that there is enough land to cultivate Jatropha on the necessary scale. Still with the same study, Boeing concluded that Algae biofuel only needs 0.0025% of the land for the production of biofuel on the necessary scale, from Jatropha feedstock, which represents the area of Ireland.

Although this particular problem can be easily overcome, there are many others that need a more profound research. Biofuels may not be a quick solution for the energy problems of the world, as many research on their properties and harvesting are still required, and in short term these may even be more expensive than petroleum fuels; however to solve our dependency in petroleum fuels, it should not be expected that this can be accomplished in a cheap or easy way.

^bThe term soot refers to impure carbon particles that result from the incomplete combustion of hydrocarbons.

^c SO_x only appears in the exhaust gases if there is any sulfur in the fuel.

B. Turbulent flow analyzes

Techniques have been developed throughout the years in order to obtain useful information and to allow predictions of turbulent flows. These techniques can be divided into two basic levels; the First-order Eddy Viscosity/diffusivity (EVM) models and the second order Reynolds Stress Models (RSM); within these models several variants exist, however the predictions obtained from this study will rely on the RSM. The RSM was chosen among other models such as the standard $k - \epsilon$ model, because it was verified that better results were obtained from the RSM, despite being more CPU expensive and more difficult to converge than EVM. It was also chosen because it is proven that RSM is more advantageous over other models, in complex 3D swirling flows such as the combustor in study, and consequently it is an efficient way to improve the simulation accuracy.¹⁵

1. Governing equations

One of the best methods of analysis turbulent flows is to write out the partial differential equations that embody the basic conservation principles, i.e, mass, momentum, energy and species; perform a Reynolds decomposition and then average the equations over time. The result of this decomposition is then the so called Reynolds Averaged Navier-Stokes (RANS) equations, and are the following:¹⁶

- Continuity:

$$\frac{\partial \bar{p}}{\partial t} + \frac{\partial}{\partial x_i}(\bar{p}\tilde{u}_i) = 0 \quad (1)$$

- Momentum:

$$\frac{\partial}{\partial t}(\bar{p}\tilde{u}_i) + \frac{\partial}{\partial x_j}(\bar{p}\tilde{u}_i\tilde{u}_j) - \frac{\partial}{\partial x_j}(\overline{p u_i'' u_j''}) - \frac{\partial}{\partial x_j} \left[\mu \left(\frac{\partial \tilde{u}_i}{\partial x_j} + \frac{\partial \tilde{u}_j}{\partial x_i} - \frac{2}{3} \partial_{ij} \frac{\partial \tilde{u}_i}{\partial x_i} \right) \right] = - \frac{\partial \bar{p}}{\partial x_i} \quad (2)$$

- Scalar transport:

$$\frac{\partial}{\partial t}(\bar{p}\tilde{\Upsilon}_\alpha) + \frac{\partial}{\partial x_i}(\bar{p}\tilde{u}_i\tilde{\Upsilon}_\alpha) + \frac{\partial}{\partial x_i}(\overline{p u_i'' \Upsilon_\alpha''}) - \frac{\partial}{\partial x_i} \left(\Gamma_\alpha \frac{\partial \tilde{\Upsilon}_\alpha}{\partial x_i} \right) = \tilde{\omega}_\alpha \quad (3)$$

In a laminar flow, the fluid stress is proportional to the rate of strain with the viscosity being a constant of proportionality. In a turbulent flow however, the turbulent stress is related to the mean rate of strain through turbulent viscosity (μ_T). This is the so called Boussinesq's hypothesis, and is represented in Eq. 4:

$$-\overline{\rho u_i'' u_j''} = \mu_T \left(\frac{\partial \tilde{u}_i}{\partial x_j} + \frac{\partial \tilde{u}_j}{\partial x_i} \right) - \frac{2}{3} \bar{\rho} k \partial_{ij} - \frac{2}{3} \mu_T \frac{\partial \tilde{u}_k}{\partial x_k} \partial_{ij} \quad (4)$$

Regarding RSM, the exact equation for the transport of Reynold's stress R_{ij} , is given by Eq. 5:

$$\frac{DR_{ij}}{Dt} = P_{ij} + D_{ij} - \varepsilon_{ij} + \Pi_{ij} + \Omega_{ij} \quad (5)$$

Where P_{ij} is the rate of production (Eq. 6), D_{ij} is the transport by diffusion (Eq. 7), ε_{ij} is the rate of dissipation (Eq. 8), Π_{ij} is the transport due to pressure-strain interactions (Eq. 9), and Ω_{ij} is the transport due to rotation (Eq. 10):

$$P_{ij} = - \left(R_{im} \frac{\partial U_j}{\partial x_m} + R_{jm} \frac{\partial U_i}{\partial x_m} \right) \quad (6)$$

$$D_{ij} = \frac{\partial J_{ijk}}{\partial x_k}, \quad \text{where } J_{ijk} = \overline{u_i' u_j' u_k'} + \overline{p' (\delta_{jk} u_i' + \delta_{ik} u_j')} \quad (7)$$

$$\varepsilon_{ij} = 2\mu \frac{\partial \overline{u_i'}}{\partial x_k} \frac{\partial \overline{u_j'}}{\partial x_k}, \quad \text{where dissipation model: } \varepsilon_{ij} = \frac{2}{3} \varepsilon \delta_{ij} \quad (8)$$

$$\Pi_{ij} = -C_1 \frac{\varepsilon}{k} (R_{ij} - \frac{2}{3} k \delta_{ij}) - C_2 (P_{ij} - \frac{2}{3} P \delta_{ij}) \quad \text{where } C_1 = 1.8 ; C_2 = 0.6 \quad (9)$$

$$\Omega_{ij} = -2\Omega_k (R_{jm} e_{ikm} + R_{im} e_{jkm}) \quad (10)$$

where depending on the indices e_{ijk} is -1 or 1, and Ω_k is the rotation vector

II. Problem setup

A. Model Construction

As occurs with many other studies, it is very difficult to obtain the blueprint of a given combustor, due to the confidentiality that the GTE manufacturing companies tend to maintain. This case was no exception; TAP kindly provided us a CFM56-3 combustor, and in order to obtain an accurate model of the combustor's geometry, a 3D scan had to be performed followed by a CAD design. The 3D scanning device used was the Artec Spider, from Artec group, which was provided by UBI. This device has an outstanding accuracy for small objects, and offers unlimited possibilities in reverse engineering. Overall the scanning process was a success. Only the exit section of the combustor could not be scanned due to the fact that the turbine support structure that was attached to the combustor was not removable, which prevented the view of the scanner to that part of the combustor.

After obtaining a 3D model of the combustor through the scanning process, this cannot be used directly for meshing and simulation purposes in Ansys FLUENT due to two reasons; first this 3D model only presents a shell of the combustor, i.e, the 3D model does not have any thickness, and secondly this model even after the post-processing step, still lacks some detail which is required for the model simulation. Thus, it is necessary to perform a CAD design, with the aid of the STL format of the 3D model, exported from Artec Studio 9.2. The CAD software chosen was CATIA V5 R19, and all of the details present in the combustor were represented, including the combustor walls, the bolts that attach the combustor wall to the dome, the dome, the cooling lips/dilution holes, fuel injectors and the primary/secondary swirlers; however due to the existing symmetry, only a quarter section of this combustor will be used for simulation purposes in order to decrease the simulation time and effectively represent the four fuel injectors that supply a richer mixture, i.e, there will be one fuel injector within the five fuel injectors, present in each quarter section of the model combustor, that supplies a richer mixture. The CAD representation of the quarter section of the combustor, can be seen in figure 1.

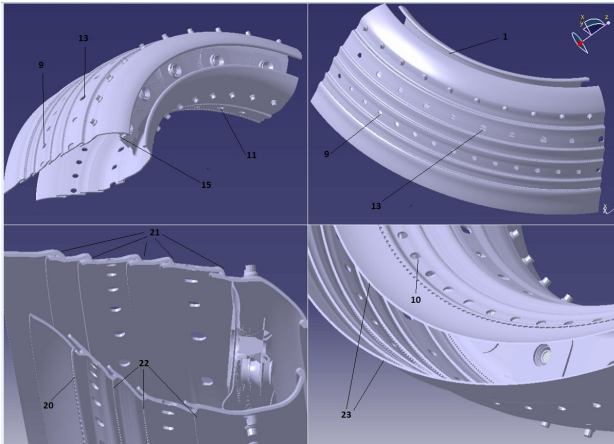


Figure 1: Quarter section CAD combustor.

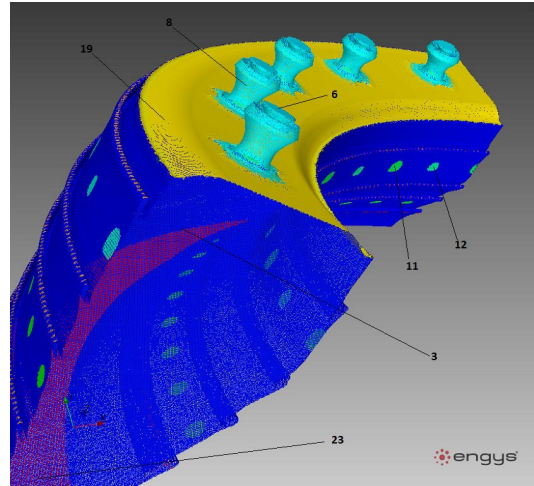


Figure 2: Meshed computational domain, after the removal of the upper volume of the dome.

1. Generation of the numerical mesh

The mesh generation was performed using HELYX-OS, which is based on snappyHexMesh. This selection was based on the work of Carlos,¹⁷ which concluded that HELYX-OS had many advantages over other mesh generating softwares like ICEM and Pointwise. Advantages include a quicker mesh generation time and a user friendly software which enables the user to better refine any given part of the mesh. HELYX-OS is an openfoam program, and as such is not available for Windows in the free version, and as so Linux was used, as it is the operating system in which HELYX-OS can be freely handled. The final results of this mesh generation resulted in a relatively fine mesh, with 2.12.300 number of cells and 7.029.105 number of faces, and with a mesh generation time of 3664 seconds.

It is also important to mention that after verifying that the upper part of the dome, in which the air first enters the combustor, was not necessary to represent because the mass flow inlets will be defined individually for the swirlers and the holes of the dome. This procedure reduced the size of the mesh in about 300.000 cells, which resulted in a significant reduction in CPU cost. The mesh after the upper part of the dome being removed, can be seen in figure 2.

B. Numerical study

The numerical study was performed using Ansys FLUENT code; the model setup is of paramount importance since these are related to the success of the simulation. Thus the energy equation was enabled since there is a temperature exchange during the combustion process; the turbulent viscous model selected was RSM, maintaining its default settings; the Discrete Ordinate (DO) is chosen for the radiation model and non-premixed is selected for the species model. Regarding this last, the specification of the fuel species name and concentration is done in the boundary tab. It is important to check if the species that are intended to introduce are presented by their thermodynamic properties, in the thermo.db file. For the present study, besides Jet-A, all of the species which compose the biofuels had to be introduced. This was done by accessing Burcat's thermodynamic data base,¹⁸ which presents a great range of the species thermodynamic properties, in the 7 term polynomial form, initially published by NASA.¹⁹ The final model that has to be enabled, is the NO_x model, otherwise FLUENT will not display any information regarding NO_x formation when the solution is calculated.

The boundary conditions were determined by dividing by four, the total \dot{m}_a and \dot{m}_f , and from the overall AFR. The typical values for GTE's operating AFR are stated by Bryn Jones,²⁰ and are between 33-40 at 100% power, and ≈ 100 at 7% power. At full power the overall AFR calculated in this work was 43.6, which represents a difference of 7% from the upper limit stated by Bryn. In order to achieve an AFR between the stated values, the total \dot{m}_a would have to be reduced; thus it was opted to use the calculated AFR as this used all of the air obtained from Pedro's work (10.36 kg/s).²¹

The first step was then to ensure that at the PZ, the AFR was at stoichiometric conditions. The \dot{m}_a that enters the PZ is done through the primary and secondary swirlers, and as so its \dot{m}_a can then be determined. Knowing the overall AFR and fuel flow, it is possible to determine the total \dot{m}_a , and then calculate the total cooling \dot{m}_a , by subtracting the PZ \dot{m}_a from the total \dot{m}_a . It was then necessary to distribute this cooling \dot{m}_a , through the boundary conditions. The determination of which percentage to apply in each boundary was only possible through an extensive trial and error approach through the simulations, in which the aim was to achieve the exit temperature reported by Pedro.²¹ Once this exit temperature was achieved, the percentage of cooling air that is applied to each boundary was then known. It is important to note that this trial and error approach was performed burning Jet-A as fuel, at full power. The boundary conditions for the remaining power settings were then similarly determined from this reference.

III. Results

A. Energy extracted

The energy extracted from the biofuels was calculated using Eq. 11, and the LHV of the biofuels. The energy extracted comes in the form of power output [kW], while burning a constant \dot{m}_f , which corresponds to the \dot{m}_f of Jet-A, at full power. The results are presented in figure 3, and it can be instantly noticed that all of the biofuel have a lower power output, when compared to Jet-A. This is expected as biofuels have a lower combustion enthalpy, which means that more biofuel is needed to produce the same amount

of energy, from that obtained from kerosene. Nevertheless, only a slight decrease is verified with *Jatropha* and *Sunflower* biofuel ($\approx 7.5\%$), however a very significant power output decrease can be noticed with *algae* biofuel ($\approx 30.4\%$). This fact drifts of course by the quality of the fuel, which hugely depends on the production conditions of the biofuel.²² Every time a new study is made to improve a given biofuel, this goal is generally achieved, and in fact, regarding *jatropha* biofuel there are several older studies which report a LHV in the order of 34.4 MJ/kg, and for this study, the LHV of *jatropha* biofuel was 39.5 MJ/kg, and was obtained from the work of Goyal et al.¹²

$$\dot{m}_{fuel} = \frac{P [kW]}{LHV_{fuel} [MJ/kg]} \quad (11)$$

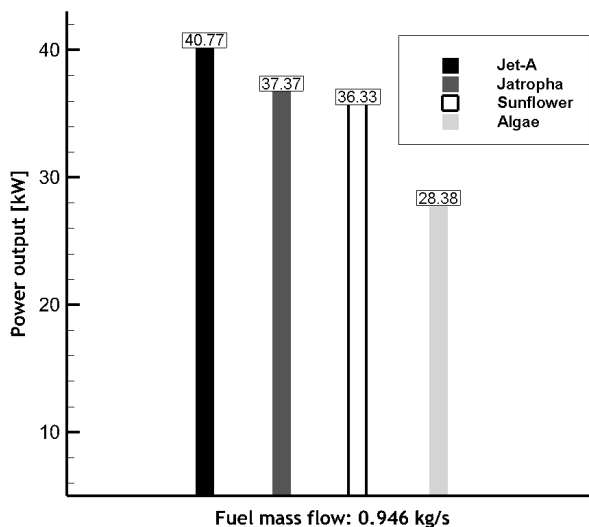


Figure 3: Energy extracted from the combustion of Jet-A vs the biofuels, at a constant \dot{m}_f .

B. Results validation

All of the results presented in this article were validated by firstly comparing the emissions calculated with the simulations while burning Jet-A, at full power, with ICAO's emissions measurements.²³ Only after obtaining reasonable results, could the other simulations take place, and therefore be considered acceptable. The results of this comparison can be seen in figure 4(a). The main issue intended to analyze in this work, is the study of NO_x emissions, and as can be seen in figure 4(a), it was the emission that presented the smallest error, which is in average 16%. It is interesting to note that at 85% power, the error was at its lowest values, accounting to only 5%. On the other hand, CO and UHC emissions presented bigger differences from ICAO's values, especially at low power settings. This was expected as high values of CO and UHC result from combustion inefficiency at low power, due to the lack of high temperature to promote complete combustion³. The bigger difference however, from ICAO's values, was due to the fact that in this study, the fuel atomization was not considered, and so the mixing that promotes enhancements in combustion efficiency is not taking place, and so these differences within CO and UHC were expected.

The combustor's exit temperature is another factor with which the results could be compared and validated. Good reference values was obtained from Pedro's work.²¹ Here, the relevant data gives respect to the exit temperature of the combustor, and here Pedro reported a value of ≈ 1650 K, at full power. For the present study, the achievement of the exit temperature was of great importance, because the boundary conditions regarding cooling air, could be determined, from a trial and error approach. The final results were very good, as it was reported, through the simulations, a value of 1582 K, which represents an error of only 4.2% from the value reported by Pedro. The predicted exit temperature results and contours, are presented in figure 4(b) and 5(a), respectively. It can be seen from image 4(b), that all of the biofuels presented lower exit temperatures when compared to Jet-A, throughout the entire ICAO LTO cycle, and that until 85% power, the values predicted were practically the same among the biofuels.

C. Emissions analyzes

All of the results presented in this section, were obtained by reporting the emission Flow rate in FLUENT, then multiplying by 1000 and dividing by the total \dot{m}_f at the inlet. The results are presented in the form g [Emissions]/kg [fuel], which makes it possible to compare with ICAO's reference data. This procedure is represented by Eq. 12:

$$\frac{\text{Emission flow rate [kg/s]} \times 1000}{\text{Inlet } \dot{m}_f \text{ [kg/s]}} = \frac{g}{kg_{fuel}} \quad (12)$$

1. Nitrogen oxides

The thermal NO_x formation is governed by the Zeldovich mechanism, and according to this theory NO_x is formed from atmospheric nitrogen at sufficiently high temperatures. These high peak temperatures are located within the PZ, but the oxidation occurs mainly in the post flame zone area, in which the concentration of the radicals O and OH are sufficient for the process to occur.²⁴ This statement can be proved by analyzing figures 5(b) and 5(c); here it can be seen that the major concentrations of NO_x are located after the flame front, and near the combustor's exit.

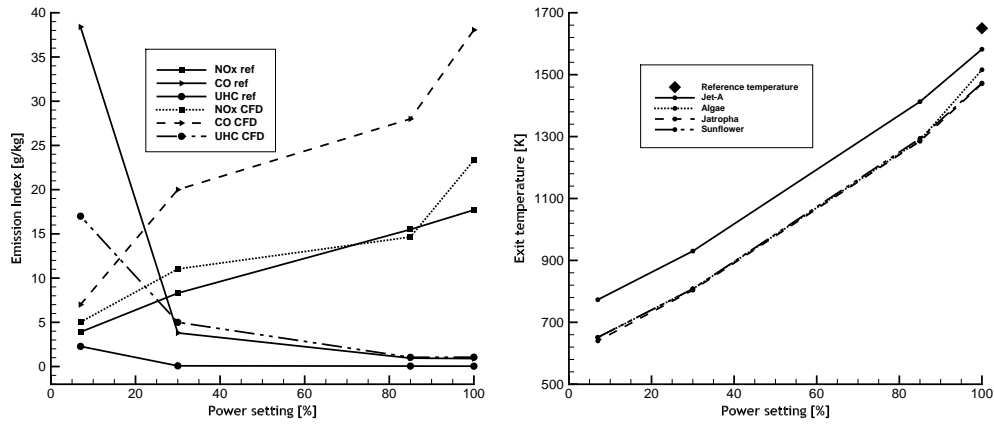
The EI NO_x results from the combustion of the fuels throughout ICAO's LTO cycle, are presented in figure 4(c)^d, and for all the biofuels, the predicted values show the correct trend of NO_x concentration increase, towards the combustor's exit. Thus, by analyzing figure 4(c) it can be noticed that all of the biofuels presented a lower EI of NO_x when compared to Jet-A. The biofuel that presented the smaller NO_x EI throughout the entire ICAO LTO cycle, was algae biofuel, and in which the biggest difference was verified at 30% power, where algae NO_x emissions were 87% smaller than those of Jet-A at the same power setting. In the other hand jatropha biofuel performed the worst among the biofuels, which at the power settings 100 and 85%, the values were very close to those of Jet-A. It can be then concluded from the NO_x emissions analyzes, that biofuels have the potential to dramatically decrease these emissions throughout all of the power settings. It is however interesting to note that as NO_x formation is strongly temperature dependent, the lower level of NO_x values may be primarily due to the lower temperature which take place on the combustor's exit, when biofuels are burned (see figure 4(b)).

2. Carbon monoxide and unburned hydrocarbons

UHC and CO emissions are associated to combustion inefficiency (or incomplete combustion from the fuel), and this last is greatly related to fuel atomization, as the small fuel particles can be more easily mixed with the air, which in turn enhances combustion efficiency. CO are generally formed due to the lack of oxygen to complete the reaction to CO_2 , and from the dissociation of this last if the mixture present in the combustion zone is stoichiometric, such as the conditions presented in the PZ⁷ (see figure 5(d)). UHC means that a waste of fuel is taking place as not all of the fuel that is injected is being burned, reaching the combustor exit in the form of drops or vapor, and as such UHC must be avoided at all cost.

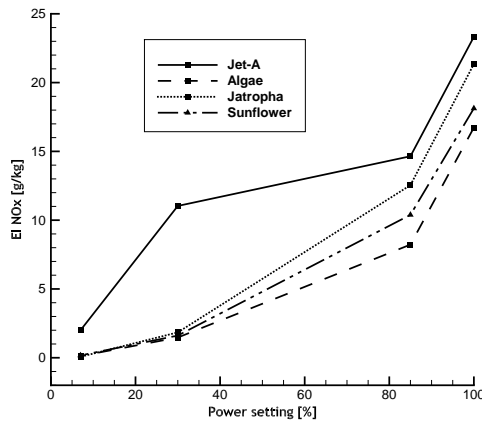
With a temperature increase it should be expected a reduction of both CO and UHC . However this behavior was not verified in all of the fuels in study, as increasing the power resulted in an increase of CO and an irregular behavior regarding UHC (figure 4(d) and 4(e)). After noticing this problem, further investigation was held in order to figure out what was happening. The answer was discovered in a project from the European Commission.²⁵ Here it is concluded that empirical models such as the RSM used in this study, although being good for NO_x predictions with a relatively low CPU cost, they cannot capture consistent trades between NO_x and other pollutants such as CO and UHC , which make these models inappropriate for the combustor's operating conditions. Moreover, the effect of flow field simplification that comes from these models, affects the prediction of different pollutants, being CO and UHC more sensitive to turbulent mixing and fluid dynamics, then NO_x emissions. The quenching effect that thrives from the cooling air near the walls, that promotes CO oxidation reactions, cannot also be captured by these models; in fact the prediction of CO emissions from these models result from the primary zone, and which entrain among the combustor's cooling, where it fails to oxidize due to low temperatures; this can be seen in figure 5(d).

^dThe EI NO_x results presented in figure 4(c) account for the total NO_x (thermal + prompt NO_x), as it was verified that the concentration of prompt NO_x only accounted for $\approx 7\%$ of the total NO_x formed in the combustor; it also did not vary that much with the type of fuel.

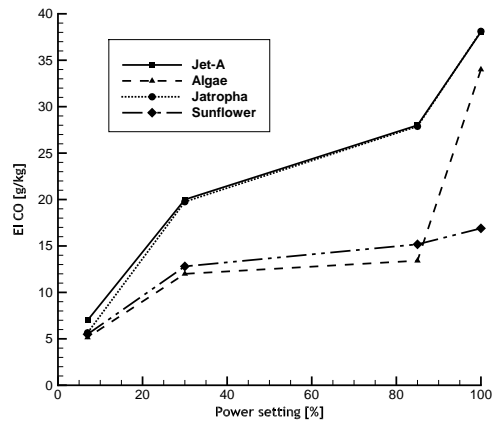


(a)

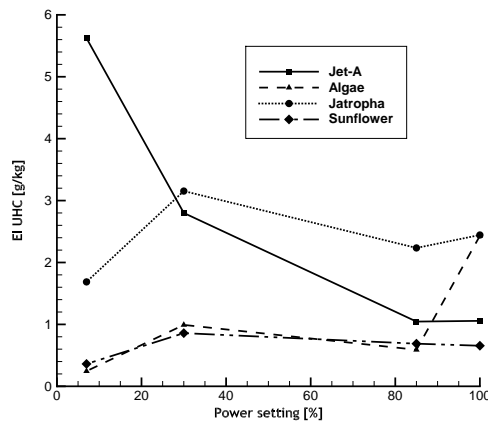
(b)



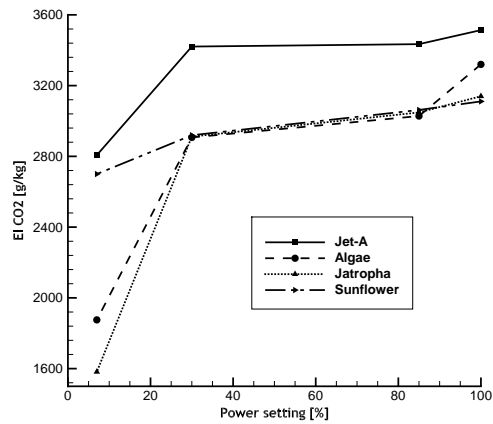
(c)



(d)



(e)



(f)

Figure 4: Results from the combustion of Jet-A and the biofuels, throughout ICAOs LTO cycle; (a) EI predictions for results validation; (b) combustor exit temperature; (c) NO_x EI; (d) CO EI; (e) UHC EI; (f) CO_2 EI.

Nevertheless all of the fuels maximum CO EI predicted throughout the cycle did not differ that much with the maximum reference values, and as so, a comparison can be made between the fuels, which is in fact presented in figure 4(d). As can be seen, by increasing the power an increase of CO emissions is taking place; the prediction of CO emissions from the combustion of jatropha biofuel proved to be identical to Jet-A through the entire cycle; both sunflower and algae biofuel presented lower CO emissions, with algae presenting the lowest emissions until 85% power, followed by a big increase of these emissions from a 85 to 100% power setting. At full power, sunflower biofuel presented the lowest CO emissions.

Regarding UHC s, the predictions are presented in figure 4(e), and only Jet-A presented the expected behavior of a decrease in emissions with a increase in power. The erroneous behavior predicted from the biofuels was verified from 7 to 30% and from 85 to 100%; from 30 to 85% the expected behavior was correctly predicted. Overall, sunflower biofuel presented the lowest UHC emissions along with algae biofuel, until this last achieved the 85% power setting. Towards full power, the combustion of algae biofuel resulted in a similar increase of UHC emissions, as that verified with CO in the same power setting. Again, Jatropha biofuel had the highest UHC emissions among the biofuels, and at which through great part of the cycle (30 to 100%), were superior than those of Jet-A. Overall, the biofuel that presented the best performance in both of these emissions was sunflower biofuel.

3. Carbon dioxide

CO_2 is a GHG and is the major contributor for global warming, as it absorbs infrared radiation emitted by the atmosphere and earth surface, preventing it from being radiated into outer space. CO_2 emissions are the result of complete combustion of fuels, and the only way of reducing these is to burn less fuel. By burning less fuel, a lower power output will be obtained, and as so the challenge for todays engineers is to design the GTE and combustor in a way that the same power output will be produced, when the \dot{m}_f is reduced; this is the so called TSFC increase, and is generally achieved from improvements in engine thermal efficiency.⁷ However, as changes in aircraft structures take a long time to happen, and are very expensive to implement in the global scale, they do not occur at the required rate to create the so needed CO_2 reduction for global warming mitigation. Thus, the easiest way in reducing these emissions is to change the fuel, because different fuels produce different amounts of CO_2 ; among all of the fuels, biofuels should be the natural choice, because as stated in section I.A, these are capable of reducing CO_2 emissions in up to 85%, and the results obtained in this study with the combustion of biofuels and CO_2 , reveal in fact a significant decrease when compared to Jet-A.

The results and contours of CO_2 prediction, are presented in figure 4(f) and figures 5(e),5(f) respectively. Regarding figures 5(e),5(f), it is important to observe that CO_2 is formed mostly in the flame zone and extends to the post-flame zone, which is in agreement with Lieuwen et al.²⁶ The emissions data presented in figure 4(f), indicate that the EI of CO_2 was the largest among the emissions considered; this is expected as CO_2 along with H_2O makes up great part of the exhaust gases. As can be seen from figure 4(f), all of the biofuels presented a reduction of CO_2 , throughout all of ICAO's LTO cycle, when compared to Jet-A. This is curious because the biofuels are burning more fuel then Jet-A, at the same power setting, and nevertheless are producing less CO_2 emissions, which demonstrates the potentiality of biofuels in reducing the major contributor to global warming; moreover the expected increase of CO_2 emissions with the power increase (since more fuel is being burned), was predicted. Still in figure 4(f), it can be verified that jatropha biofuel presented the lowest CO_2 at idle, representing $\approx 45\%$ difference from Jet-A emissions at the same power setting; at full power, sunflower biofuel had the less CO_2 emissions, presenting a $\approx 24\%$ difference from Jet-A. Over all of ICAO's LTO cycle, the biofuel that presented the greatest reduction of CO_2 emissions was jatropha biofuel, which was predicted a 20% difference from Jet-A. This value is still not near from the stated difference of 85%, however taking into account that combustion inefficiency is occurring due to the non atomization of the fuel^e, these results are already good.

IV. Conclusion

Overall, all of the biofuels presented a higher fuel consumption but this can be mitigated, by the fact that lower emissions were predicted from the biofuels, throughout all of the power cycle; all of the biofuels also presented lower combustor exit temperatures. Each of the biofuels considered presented better behavior

^eWhich would lead to a greater reduction of CO_2

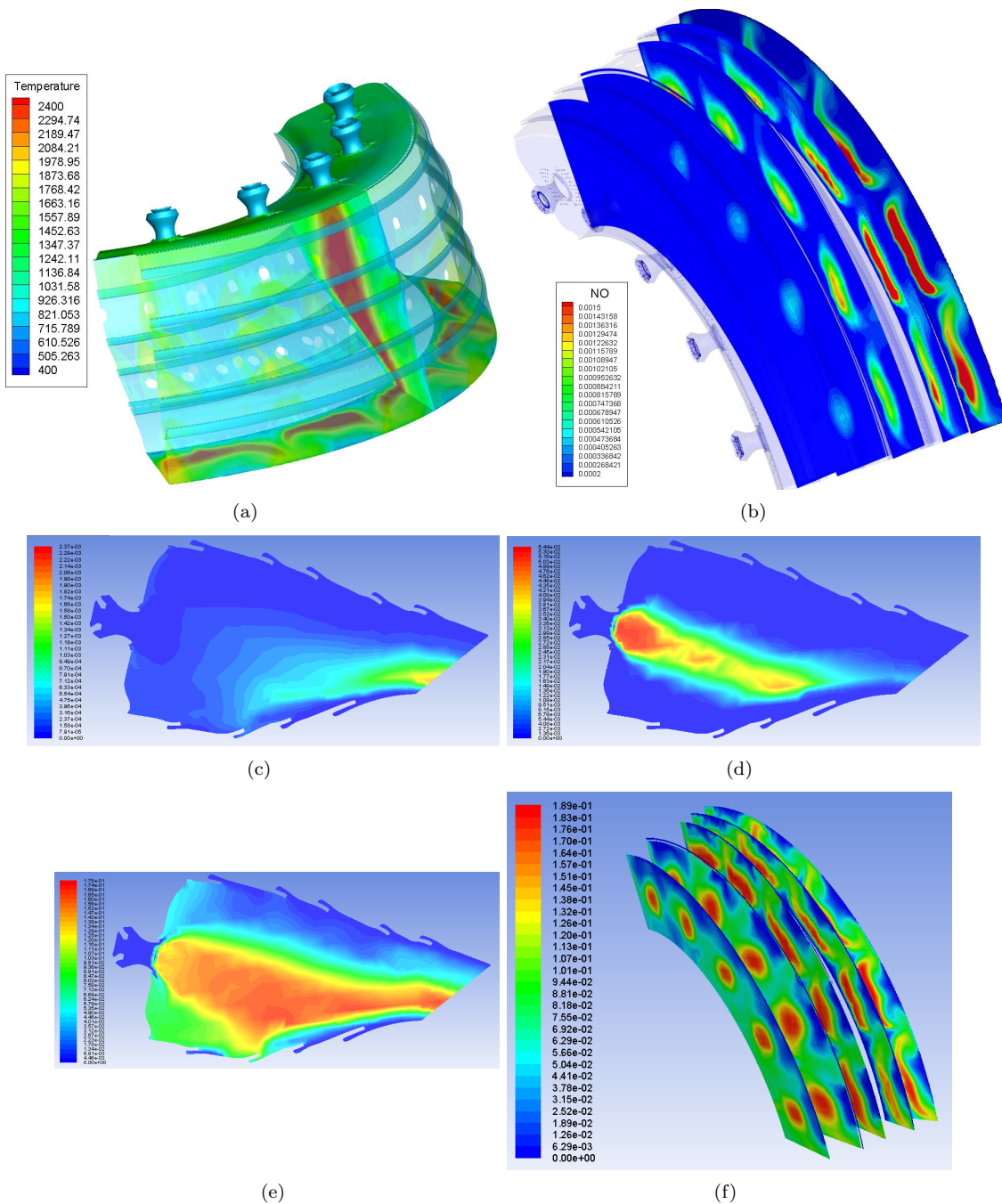


Figure 5: Contours (a) of the combustor exit temperature (K), while burning jatropha biofuel, at full power; (b) of NO_x concentration [kg/kg], while burning jatropha biofuel at full power; (c) of NO_x concentration [kg/kg], while burning algae biofuel at 85% power; (d) of CO concentration [kg/kg], while burning algae biofuel at full power; (e), (f) of CO_2 concentration [kg/kg] at 85% power, while burning sunflower and jatropha biofuel, respectively.

in some emissions than in others, and as so in the future it is necessary to weigh which would prove of more benefit. Thus, the biofuels in which were predicted a greater reduction of NO_x , CO , CO_2 and $UHCs$ emissions throughout the entire ICAO LTO cycle, were respectively algae (48%), sunflower (46%), jatropha (19%) and sunflower (76%). This last difference is of great importance as it means that little amount of fuel is being wasted; moreover due to the fact that sunflower biofuel presented the best overall behavior, it is concluded from this study that sunflower biofuel is the most suitable biofuel to replace Jet-A in a combustion point of view.

Acknowledgments

My deepest thanks to TAP for providing the combustor, which was the foundation of this work. I would also like to acknowledge Olga Skvortsova, a member of Artec support team, for all of her kind advices to solve some persistent problems that rose during the scanning phase. I am profoundly grateful to CODI, and more specially Jennifer Faustino, for enabling that this hole project of reverse engineering could gain life, as they performed a 3D print of the model combustor and offered it to UBI.

References

- ¹Rebek, A., *Fickle Rocks*, Fink Publishing, Chesapeake, 1982.
- ²*Climate change: commission proposes bringing air transport into EU emissions trading scheme*, E. Commission, 2015.
- ³A. Runge, *Aviation and emissions trading*, ICAO Council Briefing, 29 Sep. 2011.
- ⁴Petroleum, B., *British Petroleum Statistical Review of World Energy*, Providence, RI, USA, 2006.
- ⁵*Alternative jet fuels*, 2006, [A supplement to Chevrons Aviation Fuels Technical Review].
- ⁶R. E. Bailis and J. E. Baka, *Greenhouse gas emissions and land use change from jatropha curcas based jet fuel in brazil*, *Environmental science & technology*, vol. 44, no. 22, pp. 8684–8691, 2010.
- ⁷A. H. Lefebvre and D. R. Ballal, *Gas turbine combustion*, CRC Press, 2010.
- ⁸H. I. H. Saravanamuttoo, G. F. C. Rogers, and H. Cohen, *Gas turbine theory*, Pearson Education, 2009.
- ⁹P. Mass, *The breaking point*, *New York Times Magazine*, vol. 21, p. 30, 2005.
- ¹⁰D. Daggett, O. Hadaller, R. Hendricks, and R. Walther, *Alternative fuels and their potential impact on aviation*, NASA, vol. 214365, no. 6, 2006.
- ¹¹H. Darby, P. Halteman, V. Grubinger, *Sunflowers for biofuel production*, 2014, [Online:] [http : //articles.extension.org/pages/29605/sunflowers – for – biofuel – production](http://articles.extension.org/pages/29605/sunflowers-for-biofuel-production), [Last checked:] 27.01.2016.
- ¹²P. Goyal, M. Sharma, and S. Jain, *Optimization of conversion of high free fatty acid jatropha curcas oil to biodiesel using response surface methodology*, *ISRN Chemical Engineering*, vol. 2012, 2012.
- ¹³S. D. Sanford, J. M. White, P. S. Shah, C. Wee, M. A. Valverde, and G. R. Meier, *Feedstock and biodiesel characteristics report*, Renewable Energy Group, vol. 416, pp. 1–136, 2009.
- ¹⁴Air transport Action Group, *Beginners guide to aviation biofuels*, Brochure, May 2009.
- ¹⁵Bilger, R.W., *Future progress in turbulent combustion and research*, *Progress in Energy and Combustion Science*, 26, pp. 367–380, 2000.
- ¹⁶M. Zedda, *Introduction to CFD for combustion applications*, Gas Turbine Combustion, Cranfield University, short course, 2015.
- ¹⁷C. Fonte, *Design of a Low Consumption Electric Car Prototype*, Master thesis, Universidade da Beira Interior, Portugal, 2015.
- ¹⁸A. Burcat and B. Ruscic, *Ideal gas thermodynamic data in polynomial form for combustion and air pollution use*, 2007, [Online:] Available : [http : //garfield.chem.elte.hu/Burcat/THERM.DAT](http://garfield.chem.elte.hu/Burcat/THERM.DAT), [Last checked:] 15.12.2015.
- ¹⁹A. Burcat and B. Ruscic, *Third millennium ideal gas and condensed phase thermochemical database for combustion with updates from active thermochemical tables*, Argonne National Laboratory Argonne, Israel Institute of Technology, 2005.
- ²⁰B. Jones, *Gas turbine combustor, design and development*, Gas Turbine Combustion, Cranfield University, short course, 2015.
- ²¹P. Ribeiro, *Anlise de performance da Famlia de Motores de Avio CFM56*, Master thesis, Instituto Superior de Engenharia de Lisboa, Portugal, 2015.
- ²²Adler, Paul R and Sanderson, Matt A and Boateng, Akwasi A and Weimer, Paul J and Jung, Hans-Joachim G, *Biomass yield and biofuel quality of switchgrass harvested in fall or spring*, *American Society of Agronomy, Agronomy Journal* 98.6: 1518-1525, 2006.
- ²³ICAO, *ICAO Engine Exhaust Emissions Data Bank; CFM56-3-B1*, Tech. rep., 2013.
- ²⁴Y. B. Zeldovich, *The oxidation of nitrogen in combustion and explosions*, *Acta Physicochim. URSS*, vol. 21, no. 4, pp. 557–628, 1946.
- ²⁵The European Commission, *Emicopter report summary*, 2014, [Online:] Available: [http : //cordis.europa.eu/result/rcn/143538_en.html](http://cordis.europa.eu/result/rcn/143538_en.html), [Last checked:] 12.01.2016.
- ²⁶T. C. Lieuwen and V. Yang, *Gas turbine emissions*, Cambridge University Press, vol. 38, 2013.